hep-ph/9608280
TUM-HEP-236/96
ILL-(TH)-96-4
August 1996

Ruling Out a Strongly-Interacting Standard Higgs Model

K. Riesselmann
Institut für Theoretische Physik
Technische Universität München
James-Franck-Straße
85747 Garching b. München
Germany

S. Willenbrock
Department of Physics
University of Illinois
1110 West Green Street
Urbana, IL 61801

Abstract

Previous work has suggested that perturbation theory is unreliable for Higgs- and Goldstone-boson scattering, at energies above the Higgs mass, for relatively small values of the Higgs quartic coupling $\lambda(\mu)$. By performing a summation of nonlogarithmic terms, we show that perturbation theory is in fact reliable up to relatively large coupling. This eliminates the possibility of a strongly-interacting standard Higgs model at energies above the Higgs mass, complementing earlier studies which excluded strong interactions at energies near the Higgs mass. The summation can be formulated in terms of an appropriate scale in the running coupling, $\mu = \sqrt{s}/e \approx \sqrt{s}/2.7$, so it can easily be incorporated in renormalization-group improved tree-level amplitudes as well as higher-order calculations.

I. INTRODUCTION

The electroweak interaction is a gauge theory, with the gauge symmetry spontaneously broken to that of electromagnetism. A major outstanding problem in particle physics is to discover the mechanism which breaks the symmetry. The simplest model of the symmetry-breaking mechanism is the standard Higgs model, in which a fundamental scalar field acquires a vacuum-expectation value $v = (\sqrt{2}G_F)^{-1/2} = 246$ GeV [1]. The particle content of the model is a spin-zero boson, dubbed the Higgs boson (H), and three massless Goldstone bosons (w^+, w^-, z) which are ultimately absorbed by the weak gauge bosons.

It has been established that the standard Higgs model exists only up to a cutoff energy Λ at or before which the model must be subsumed by a more fundamental theory [2]. Thus the standard Higgs model is regarded as an effective field theory, valid for energies less than Λ. The maximal allowed value of Λ decreases with increasing Higgs mass, m_R. Demanding, for consistency, that $m_R < \Lambda$ leads to an upper bound on the Higgs mass [3].

In this paper we address the question of whether the standard Higgs model can be strongly interacting at energies and Higgs masses less than the cutoff Λ. By "strongly interacting" we mean that the Higgs self-coupling, λ, is so large that perturbation theory is unreliable. There are two scenarios which yield a large value for the Higgs coupling: (i) The running coupling $\lambda(\mu)$ increases with increasing scale μ, leading to a strong coupling at energies above the Higgs mass; (ii) A Higgs mass, m_R, much larger than the vacuum-expectation value, $v = 246$ GeV, results in a large coupling $\lambda(m_R) \equiv m_R^2/2v^2$. Since the Higgs model is constrained by the cutoff Λ, the two possibilities lead to the following questions:

- Can the running coupling $\lambda(\mu)$ become strong for energies $\sqrt{s}$ in the range $m_R < \sqrt{s} < \Lambda$?

- Can $\lambda(m_R)$ be strong for values of the Higgs mass m_R below the cutoff Λ?

The first question is related to high-energy processes such as Higgs- and Goldstone-boson scattering. The second question can be investigated in the context of Higgs-boson decays.

Since both of these processes have been calculated at next-to-next-to-leading order in perturbation theory, they are appropriate indicators of the reliability of perturbation theory.

A popular way to model the cutoff Λ is to use a lattice with a finite lattice spacing a [3]. For a review of early work, we refer to Ref. [2], whereas a more current set of references is given in, for example, Refs. [4,5]. Using such an approach, the cutoff Λ is proportional to a^{-1}. When lattice-spacing effects on physical quantities are small, the model is equivalent to the standard Higgs model in the continuum. When lattice-spacing effects are large, the standard Higgs model ceases to exist as an effective field theory. This observation can be used to establish an upper bound on the Higgs mass.

Using the condition that the inverse lattice spacing be greater than twice the Higgs mass ($a^{-1} > 2m_R$), Lüscher and Weisz [6,7] determined an upper bound on $\lambda(m_R)$ of 3.2, corresponding to an upper bound on the Higgs mass of 630 GeV. A subsequent study [4] found a similar upper bound on $\lambda(m_R)$. Alternative formulations of the lattice action can increase the bound slightly [4,5]. Lüscher and Weisz argued that perturbation theory is reliable for a Higgs coupling of $\lambda(m_R) = 3.2$. They based their statement on observations regarding three perturbative observables: (i) Such a value of $\lambda(m_R)$ yields a perturbative Higgs width which is much less than its mass, (ii) Two-loop perturbative cross sections at threshold in the symmetric phase of the model are apparently convergent for such a coupling, and (iii) This coupling is less than the perturbative unitarity bound* on λ. They therefore concluded that there is no strongly-interacting Higgs model in which the cutoff is substantially greater than the Higgs mass.

Recent perturbative studies of high-energy Higgs- and Goldstone-boson scattering in the broken phase of the model have led to a different conclusion [8–11]. Considering the high-energy limit, the relevant coupling of these observables is the running coupling $\lambda(\mu)$, where

*The perturbative unitarity "bound" is not an absolute bound on the possible value of λ (or the Higgs mass), but rather the value above which the coupling is strong. In contrast, the lattice bound on the coupling is truly a bound, in the sense that the standard Higgs model cannot exist as an effective field theory if the coupling exceeds this value.

μ is of the order of the center-of-mass energy, $\sqrt{s}$. Using a variety of criteria, all high-energy studies found that the two-loop high-energy perturbative amplitudes do not converge satisfactorily for $\lambda(\sqrt{s}) \gtrsim 2.0 - 2.3$. For example, Durand, Lopez, and Johnson argued that perturbation theory is unreliable for $\lambda(\sqrt{s})$ as low as 2.0 [8]. This conclusion was based on a one-loop analysis of partial-wave unitarity in Higgs- and Goldstone-boson scattering, and on the lack of convergence of the perturbation series. Using a variety of additional criteria to judge the convergence of the perturbative series, subsequent analyses at two loops have only served to reinforce this conclusion [9–11]. Since the running coupling $\lambda(\sqrt{s})$ can attain a value of $2.0 - 2.3$ for values of $\sqrt{s} < \Lambda$, the standard Higgs model could be strongly interacting at energies above the Higgs mass but below the cutoff Λ.

In this paper we reinvestigate the perturbative behaviour of the high-energy Higgs- and Goldstone-boson scattering. We introduce a summation procedure which shifts the value of the coupling at which perturbation theory becomes unreliable to $\lambda \approx 4.0$. Requiring that the energy $\sqrt{s}$ be less than the cutoff Λ, the perturbative bound $\lambda \approx 4.0$ is large enough to ensure the absence of a strongly-interacting Higgs sector at high energies. Thus our summation procedure restores the convergence of perturbation theory at energies above the Higgs mass but below the cutoff Λ. This is a new result, and complements the result of Lüscher and Weisz on the impossibility of a strong Higgs coupling at $\mu \approx m_R$. We conclude that the possibility of a strongly-interacting standard Higgs model is eliminated at all energies.

Our summation procedure is based on identifying a certain class of Feynman diagrams which can be summed by an appropriate scale μ in the running coupling $\lambda(\mu)$. Calculating high-energy Higgs- and Goldstone-boson scattering, all previous analyses have implicitly or explicitly chosen $\mu = \sqrt{s}$ [8–10], or have varied the scale about this value [11]. We argue that a better scale is $\mu = \sqrt{s}/e \approx \sqrt{s}/2.7$. This scale corresponds to a summation of a universal nonlogarithmic term which accompanies the leading logarithms in the Higgs- and Goldstone-boson scattering diagrams. We show that this summation greatly improves the convergence of perturbation theory: the coefficients of the perturbative series are greatly

reduced as seen up to two loops, and the scale dependence is significantly reduced when varying μ around $\sqrt{s}/e$ (rather than $\sqrt{s}$).

The remainder of the paper is organized as follows. In section 2 we reanalyse Higgs- and Goldstone-boson scattering up to two loops, and argue for the appropriate scale μ in the running coupling $\lambda(\mu)$. We consider the convergence of perturbation theory and the partial-wave unitarity of these scattering amplitudes with this improved choice of scale. We derive the value of the running coupling for Higgs- and Goldstone-boson scattering at the cutoff Λ, and find that it is within the range of validity of perturbation theory. In section 3 we briefly review the Higgs decay amplitude at two loops. We show that for the decay amplitude, the natural scale $\mu = m_R$ is unaffected by our summation procedure. The value of $\lambda(m_R) \approx 4.0$ at which perturbation theory becomes unreliable in Higgs decays remains unchanged from a previous analysis. In section 4 we discuss some phenomenological consequences of our work for scattering cross sections. We summarize our results in section 5.

II. HIGGS- AND GOLDSTONE-BOSON SCATTERING

An estimate of the value of the Higgs running coupling $\lambda(\mu)$ at which perturbation theory becomes unreliable can be obtained from the evaluation of $2 \to 2$ scattering processes in the standard Higgs model at high energy ($s \gg m_R^2$) [12,13,8–11]. The basis for such analyses is the generic high-energy scattering amplitude of Higgs and Goldstone bosons, $a(s,t,u)$. Up to two loops the relevant Feynman scattering diagrams are shown in Fig. 1. Including the combinatoric factors, the unrenormalized scattering amplitude is

$$\begin{aligned} a_0(s,t,u) \overset{s\gg m_R^2}{=} & -2\lambda_0 - \lambda_0^2 \left[(10+2n_g)B(s) + 4B(t) + 4B(u) \right] \\ & -\lambda_0^3 \Big[(38+16n_g+2n_g^2)[B(s)]^2 + 8[B(t)]^2 + 8[B(u)]^2 \\ & \qquad +(104+24n_g)A(s) + (56+8n_g)A(t) + (56+8n_g)A(u) \Big] \\ & +O(\lambda_0^4) + O(m_R^2/s)\,. \end{aligned} \tag{2.1}$$

Here $n_g = 3$ is the number of Goldstone bosons, and the quantity λ_0 denotes the bare Higgs quartic coupling. The functions A and B correspond to the Feynman diagrams depicted in

Fig. 1: B is the one-loop "bubble" diagram, and A is the two-loop "acorn" diagram [14].

The renormalized amplitude is

$$a(s,t,u) = \left(Z_w^{1/2}\right)^4 a_0(s,t,u)\Big|_{\lambda_0=\lambda+\delta\lambda} , \tag{2.2}$$

where Z_w is the wavefunction renormalization of the Goldstone-boson fields and $\delta\lambda$ is the coupling counterterm.

It is standard in both lattice and continuum calculations to express the renormalized amplitude in terms of the Higgs mass, m_R, and the coupling [6,8,15]†

$$\lambda(m_R) \equiv \frac{1}{2}\frac{m_R^2}{v^2}, \tag{2.3}$$

where v is the vacuum-expectation value of the Higgs field, defined by $v \equiv (\sqrt{2}G_F)^{-1/2} = 246$ GeV, with G_F extracted from some low-energy weak process, such as muon decay. Up to numerically small corrections (see Appendix A), m_R corresponds to the physical Higgs mass. The wavefunction renormalization constant and the coupling counterterm are known up to two loops [14,16].

In the limit $s \gg m_R^2$, the physical $2 \to 2$ scattering amplitudes of the Higgs and Goldstone bosons are related to the generic high-energy amplitude $a(s,t,u)$ in the following way:

$$A_{WW\to ZZ} = \frac{Z_H}{Z_w}A_{HH\to ZZ} = \frac{Z_H}{Z_w}A_{HH\to WW} = a(s,t,u)\,, \tag{2.4}$$

$$A_{WW\to WW} = a(s,t,u) + a(t,s,u)\,, \tag{2.5}$$

$$A_{ZZ\to ZZ} = \frac{Z_H^2}{Z_w^2}A_{HH\to HH} = a(s,t,u) + a(t,s,u) + a(u,t,s)\,. \tag{2.6}$$

The wavefunction renormalization Z_H of the external Higgs field is given in [9,16]. A detailed investigation of the perturbative behaviour of the different channels is carried out in Ref. [10].

Of particular interest is the approximate SO(4) singlet scattering amplitude $\tilde{a}^0$. It is the s-wave projection of this amplitude which yields the strongest unitarity bound in perturbation

---

†To make contact with the notation of Refs. [6,7] and of most subsequent lattice work, note that $g_R \equiv 6\lambda(m_R)$.

theory. At tree level, $\tilde{a}^0$ equals the SO(4) singlet eigenamplitude a^0 considered by Lee, Quigg, and Thacker [13]. The corresponding tree-level SO(4) singlet eigenstate is

$$\chi^0 = \frac{1}{\sqrt{8}}(2w^+w^- + zz + HH)\,, \tag{2.7}$$

and the tree-level eigenamplitude $a^0(\chi^0 \to \chi^0)$ is expressible in terms of the generic function $a(s,t,u)$:

$$a^0 = 2a(s,t,u) + \frac{3}{4}a(t,s,u) + \frac{1}{4}a(u,t,s)\,. \tag{2.8}$$

At one loop and beyond, the eigenstate χ^0 mixes with the isospin-singlet component of the SO(4) nonet states [8,9]. The resulting eigenstate $\tilde{\chi}^0$ determines the modified eigenamplitude $\tilde{a}^0$. An appropriately-normalized integral over the scattering angle yields the $J = 0$ partial-wave-projected eigenamplitude $\tilde{a}^0_0$, the usual s-wave amplitude.

Including the two-loop corrections [9], we can write the renormalization-group improved s-wave eigenamplitude $\tilde{a}^0_0$ in terms of the running coupling $\lambda(\mu)$. Not specifying a particular choice of μ, we find:

$$\tilde{a}^0_0 = -\left(\frac{\mu^2}{m_R^2}\right)^{\gamma} \frac{3}{8\pi}\lambda(\mu)\left\{1 + \frac{\lambda(\mu)}{16\pi^2}\left[12\ln\frac{s}{\mu^2} - 22.27 - 6\pi i\right]\right.$$
$$\left. + \left(\frac{\lambda(\mu)}{16\pi^2}\right)^2\left[144\ln^2\frac{s}{\mu^2} + (-691.1 - 144\pi i)\ln\frac{s}{\mu^2} + 1012.3 + 821.6i\right]\right\}\,. \tag{2.9}$$

The definition of the running coupling $\lambda(\mu)$ is given in Appendix B. The renormalization group is used to evolve the coupling from the Higgs mass, see Eq. (2.3), up to a scale $\mu > m_R$. The only explicit dependence of the amplitude on m_R occurs in the overall factor associated with the anomalous dimension γ of the eigenstate $\tilde{\chi}^0$. At one loop $\gamma = 0$, and at two loops γ is numerically small [9]:

$$\gamma = -12\left(\frac{11}{2} - \pi\sqrt{3}\right)\left(\frac{\lambda}{16\pi^2}\right)^2 = -2.8 \times 10^{-5}\lambda^2\,. \tag{2.10}$$

Since we are concerned with values of $\lambda(\mu) < 10$, we may approximate $\gamma \approx 0$ throughout our analysis. The eigenamplitude $\tilde{a}^0_0$ then has no explicit dependence on m_R: it depends only on the running coupling $\lambda(\mu)$ and the scale μ. It is therefore an ideal observable to derive perturbative upper bounds on the running coupling in the limit $s \gg m_R^2$.

A. The choice of the scale μ

The scale μ should be chosen such that the logarithms in the amplitude, Eq. (2.9), are small, in order to avoid large coefficients in the perturbative expansion. By inspection of Eq. (2.9), we see that μ should be of order $\sqrt{s}$. This choice corresponds to a summation of the leading logarithms into the running coupling. This observation has led to the scale $\mu = \sqrt{s}$ becoming the standard in calculations of Higgs- and Goldstone-boson scattering. Using this scale, one finds that the perturbative expansion of $\tilde{a}_0^0$ becomes unreliable for the surprisingly-low value $\lambda(\sqrt{s}) = 2.0 - 2.3$ [8–11], as discussed in the Introduction.

We argue that a more appropriate choice is $\mu = \sqrt{s}/e \approx \sqrt{s}/2.7$. We begin by reviewing the calculation of $a(s,t,u)$ at one loop. Starting from Eq. (2.2), the contributions to the renormalized amplitude are the bubble diagram B (Fig. 1, top), the wavefunction renormalization Z_w, and counterterms:

$$\begin{aligned} a(s,t,u) = &-2\lambda(\mu) - \lambda^2(\mu)\,[16B(s) + 4B(t) + 4B(u)] \\ &+ \text{counterterms} + \text{ wavefunction renorm. }. \end{aligned} \tag{2.11}$$

The one-loop renormalization-group logarithms, $\ln(p^2/\mu^2)$, arise solely from the bubble scattering diagrams ($p^2 = s, t$, or u), with the internal lines of the bubble representing either Higgs- or Goldstone-boson propagators. In the high-energy limit, $s \gg m_R^2$, the mass of the Higgs boson can be neglected, so the evaluation of the bubble diagram $B(p^2)$ involves only massless propagators. In dimensional regularization ($D = 4 - 2\epsilon$), one finds at one loop

$$B(p^2) = \frac{1}{16\pi^2}\left(\Delta + \ln\frac{\mu^2}{-p^2} + 2 + O(\epsilon)\right), \tag{2.12}$$

where p^2 is the four-momentum squared flowing through the bubble, and

$$\Delta \equiv \frac{1}{\epsilon} - \gamma + \ln 4\pi \tag{2.13}$$

is divergent in four dimensions ($\epsilon = 0$). The Euler constant is denoted by γ.

Evaluating the renormalized amplitude $a(s,t,u)$ according to Eq. (2.11), all the Δ's are cancelled by the counterterms, yielding a finite result. However, the constant 2 appearing in

Eq. (2.12) is *not* cancelled in the renormalized amplitude. This is because the counterterms are calculated at "low" energies: $p^2 = m_R^2$ in the case of Higgs counterterms, $p^2 = 0$ for Goldstone-boson quantities. Hence one cannot neglect the Higgs mass in the calculation of the counterterms, so the counterterms do not involve massless bubble diagrams (except for those which involve two massless Goldstone bosons). As a result, the constant which accompanies the divergence Δ varies from diagram to diagram when calculating the low-energy counterterms (see Appendix C), unlike the universal constant 2 which appears in *all* high-energy scattering bubble diagrams.

Putting together the various contributions, the renormalized one-loop amplitude may be written

$$a(s,t,u) = -2\lambda(\mu) + \frac{\lambda^2(\mu)}{16\pi^2}\left[\beta_0\left(\ln\frac{\mu^2}{s} + 2\right) + (10+2n_g)i\pi - 4\ln\frac{\sin^2\theta}{4} - 4n_g - 1.35\right] . \quad (2.14)$$

The coefficient of the logarithm, $\ln(\mu^2/s)$, is the one-loop beta-function coefficient, $\beta_0 = 18 + 2n_g = 24$, and we maintain the association of the constant 2 with the logarithm as suggested by Eq. (2.12). The other terms appearing in (2.14) have the following origin: the imaginary part is from the s-channel bubble diagrams, the angular dependence is from the t- and u-channel diagrams (where $t, u = -s(1 \pm \cos\theta)/2$, and θ is the center-of-mass scattering angle), and the term $-4n_g - 1.35$ originates from counterterms and wavefunction renormalization. The crossed amplitude, $a(t,s,u)$, has the same β_0 term as $a(s,t,u)$, but its imaginary part as well as its angular dependence are different. This leads to the universal appearance of the term $\beta_0(\ln(\mu^2/s) + 2)$ in all high-energy amplitudes listed in Eqs. (2.4)–(2.6).

The two-loop Feynman scattering diagrams which contribute to the amplitude are shown in Fig. 1 (bottom row), and their analytical results are given in Appendix D. There are two different topologies: a chain of two bubbles, $[B(p^2)]^2$, and the "acorn" diagram, $A(p^2)$, which consists of a bubble subdiagram inserted at a vertex of a bubble diagram. Each class of diagrams contributes to the leading logarithm at two loops, $\ln^2(\mu^2/s)$. The chain of two bubbles clearly has a 2 associated with each logarithm since it is the square of the one-loop

bubble diagram. According to Eq. (2.1) and taking $n_g = 3$, roughly half of the two-loop leading logarithms come from the chain of two bubble diagrams, $B^2(p^2)$. The other half of the two-loop leading logarithms comes from the acorn diagram, $A(p^2)$, which is more subtle: the bubble subdiagram of $A(p^2)$ does have a 2, but the energy scale appearing in its logarithm is not s, but rather is an integration variable which is integrated over when the subdiagram is inserted into the full two-loop diagram $A(p^2)$. The remaining second loop integration then becomes a modified bubble diagram, with a momentum-dependent vertex (due to the bubble subdiagram). This loop integration does not simply yield a constant 2.

The situation is similar at three loops and beyond. At n loops there is always a topology which is a product of n bubbles. This class of diagrams has the maximal number of 2's connected with the leading logarithm. Next there are topologies which have $n-1$ bubbles, with the final integration being a modified bubble integral. Then there are topologies with $n-2$ bubbles, and so on. Starting at three loops, there also exist nonplanar graphs which cannot be naturally viewed as being constructed from bubble graphs. Yet their weight is expected to be small compared to the numerous bubble related contributions to the complete set of n-loop diagrams.

The universality of the term $\beta_0(\ln(\mu^2/s) + 2)$ suggests that the scale μ should be chosen to eliminate both the logarithm and the constant. Hence we advocate

$$\mu = \frac{\sqrt{s}}{e} \approx \frac{\sqrt{s}}{2.7}\,, \tag{2.15}$$

in contrast to the usual choice $\mu = \sqrt{s}$. Our choice of scale amounts to summing the constant 2 along with the leading logarithm to all orders in perturbation theory. At two loops and beyond, the new scale also reduces the finite contributions coming from the $O(\epsilon^n)$ terms; see Appendix E. Since none of the other terms in Eq. (2.14) are proportional to β_0, it is inappropriate to choose the renormalization-group scale μ to sum any of them.

B. Testing the new scale

A concern is that the scale $\mu = \sqrt{s}/e$ may not be an appropriate choice for the next-to-leading logarithms, which first appear at two loops. A "bad" choice of scale could result in a large two-loop coefficients. To investigate this aspect, we compare the perturbative expansions of the eigenamplitude $\tilde{a}_0^0$ at next-to-next-to-leading order, using the scales $\mu = \sqrt{s}$ and $\mu = \sqrt{s}/e$. Choosing the scale $\mu = \sqrt{s}$, one obtains from Eq. (2.9) (approximating $\gamma = 0$)

$$\tilde{a}_0^0 = -\frac{3}{8\pi}\lambda(\sqrt{s})\left\{1 + \frac{\lambda(\sqrt{s})}{16\pi^2}\left[\,-22.27 - 6\pi i\,\right] + \left(\frac{\lambda(\sqrt{s})}{16\pi^2}\right)^2\left[\,1012.3 + 821.6i\,\right]\right\}\,, \qquad (2.16)$$

where $\lambda(\sqrt{s})$ is the three-loop running coupling evaluated at $\mu = \sqrt{s}$. The new scale $\mu = \sqrt{s}/e$ yields

$$\tilde{a}_0^0 = -\frac{3}{8\pi}\lambda(\sqrt{s}/e)\left\{1 + \frac{\lambda(\sqrt{s}/e)}{16\pi^2}\left[\,1.73 - 6\pi i\,\right] + \left(\frac{\lambda(\sqrt{s}/e)}{16\pi^2}\right)^2\left[\,206.1 - 83.1i\,\right]\right\}\,, \qquad (2.17)$$

where the three-loop running coupling is evaluated at $\mu = \sqrt{s}/e$. We find that the summation of the 2's greatly reduces the size of the coefficients of the perturbative amplitude. Furthermore, the value of the running coupling at $\mu = \sqrt{s}/e$ is *less* than at $\mu = \sqrt{s}$, leading to a further improvement in the convergence of perturbation theory. The above results support the improved scale at the leading-log level and also suggest that it is the appropriate scale at the subleading level.

C. Upper perturbative bound on the running coupling

We now attempt to quantify the value of $\lambda(\sqrt{s}/e)$ at which perturbation theory becomes unreliable. There are three criteria we can use to judge the convergence of perturbation theory: (i) The size of the radiative corrections should be small; (ii) The scale dependence should decrease with increasing order in perturbation theory; (iii) The amplitude should not violate perturbative unitarity by a large amount.

We begin by investigating the size of the radiative corrections and the scale dependence of the amplitude. In Fig. 2 we show the real and imaginary parts of $\tilde{a}_0^0$ at leading order

(LL), next-to-leading order (NLL), and next-to-next-to-leading order (NNLL), for various values of $\lambda(\sqrt{s}/e)$, as a function of the renormalization scale μ (scaled by $\sqrt{s}$). Table I contains a translation of the values of $\lambda(\sqrt{s}/e)$ to the conventional quantity $\lambda(\sqrt{s})$, and to some corresponding pairs of $(m_R, \sqrt{s})$. A smaller Higgs mass requires a larger $\sqrt{s}$ to obtain a given value of $\lambda(\sqrt{s}/e)$ since the running coupling must evolve over a larger energy range to achieve the same magnitude of the coupling.

As is evident from Fig. 2, the size of the radiative corrections is greatly reduced for the scale $\mu = \sqrt{s}/e$ in comparison with the scale $\mu = \sqrt{s}$. Furthermore, the scale dependence is much less when the scale is varied about $\mu = \sqrt{s}/e$ rather than $\mu = \sqrt{s}$. These observations apply to both the real and imaginary parts of the amplitude. They support our finding that the appropriate scale for Higgs- and Goldstone-boson scattering, at energies large compared with the Higgs mass, is $\mu = \sqrt{s}/e$. Judging from the scale dependence, it seems that perturbation theory begins to break down around $\lambda(\sqrt{s}/e) = 4.0$. Note, however, that even for this value of λ the magnitude of the radiative corrections is not very large, so the size of the corrections does not appear to be a good indication of the reliability of perturbation theory.

A third method of judging the convergence of perturbation theory is to check the nonperturbative requirement that the eigenamplitude must lie in or on the unitarity circle. Plotting an Argand diagram, we show in Fig. 3 the value of the one-loop and two-loop RG improved s-wave eigenamplitude $\tilde{a}_0^0$ when taking $\mu = \sqrt{s}/e$ (see Eq. (2.17)), indicating various values of the coupling $\lambda(\sqrt{s}/e)$ (long dashed curves). Also shown is the eigenamplitude when taking $\mu = \sqrt{s}$ (see Eq. (2.17)) [8,9], indicating various values of $\lambda(\sqrt{s})$ (short dashed curves).[‡] At leading-order the two approaches coincide (dotted curve) since the choice of μ has no influence on the tree-level coefficient. The fact that, for the same value of λ, the amplitudes

[‡]The values in the case $\mu = \sqrt{s}$ are not identical to those in Refs. [8,9] since a slightly different initial condition was used for the renormalization-group equation in [8,9] than is used here. That initial condition leads to the amplitude straying slightly further from the unitarity circle for a given value of $\lambda(\sqrt{s})$.

with the scale $\mu = \sqrt{s}/e$ lie closer to the unitarity circle is another way of demonstrating the improved convergence of perturbation theory with this scale. We may also use this plot to again estimate the value of the coupling at which perturbation theory becomes unreliable. The next-to-next-to-leading-order amplitude begins to stray uncomfortably far from the unitarity circle for $\lambda(\sqrt{s}/e) \approx 4$. This yields a perturbative upper bound on the running coupling which is in agreement with our findings above.

Previous analyses, using the scale $\mu = \sqrt{s}$, concluded that perturbation theory becomes unreliable for $\lambda(\sqrt{s}) = 2.0 - 2.3$ [8–11]. This corresponds to $\lambda(\sqrt{s}/e) = 1.6 - 1.8$. Figs. 2 and 3 suggest that perturbation theory is very convergent for this range of $\lambda(\sqrt{s}/e)$. Choosing $\mu = \sqrt{s}/e$ we conclude that both scale dependence and unitarity indicate that perturbation theory becomes unreliable for $\lambda(\sqrt{s}/e) \approx 4$. This value is comparable to the simple tree-level unitarity bound of $\lambda < 4\pi/3 \approx 4.2$ based on $|\mathrm{Re}\, a_0^0| < 1/2$ [12,13,6,17].

D. The absence of a strongly-interacting Higgs sector at high energies

We now ascertain the largest value of $\lambda(\sqrt{s}/e)$ attainable with the constraint $\sqrt{s} < \Lambda$ in order to answer the question posed in the Introduction: Can the running coupling be strong for energies $\sqrt{s}$ in the range $m_R < \sqrt{s} < \Lambda$? It is impossible to define the cutoff Λ precisely, but Lüscher and Weisz have argued that the effective lattice cutoff lies roughly between a^{-1} and $2a^{-1}$, by studying the cutoff effects on Goldstone-boson scattering above the Higgs mass [7].[§] The cutoff effects on Goldstone-boson scattering at $2a^{-1}$ are on the order of ten percent [4,7]. The authors found that the relationship between the lattice spacing a and the renormalized coupling $\hat{\lambda}(m_R) \equiv \lambda(m_R)/16\pi^2$ is given approximately by the semi-perturbative two-loop formula

$$\ln \frac{1}{m_R a} = \frac{1}{\beta_0 \hat{\lambda}(m_R)} + \frac{\beta_1}{\beta_0^2} \ln[\beta_0 \hat{\lambda}(m_R)] - \ln C \tag{2.18}$$

[§]In Ref. [6,7], a^{-1} is denoted by Λ. We use Λ to denote the cutoff, which is only proportional to a^{-1}.

where $\beta_0 = 24$, $\beta_1 = -312$ are the one- and two-loop beta-function coefficients, and $\ln C = 1.9$ is a constant which has been obtained nonperturbatively [6,7]. (Ref. [4] finds a slightly smaller value, $\ln C = 1.445$.) The consistent solution of the two-loop renormalization-group equation for $\hat{\lambda}(\mu) \equiv \lambda(\mu)/16\pi^2$ is [11]

$$\frac{\hat{\lambda}(m_R)}{\hat{\lambda}(\mu)} = 1 - \beta_0 \hat{\lambda}(m_R) \ln \frac{\mu}{m_R} + \frac{\beta_1}{\beta_0} \hat{\lambda}(m_R) \ln \frac{\hat{\lambda}(m_R)}{\hat{\lambda}(\mu)} \; . \tag{2.19}$$

Combining these two equations, we obtain an implicit relation between $\hat{\lambda}(\mu)$ and a:

$$\frac{1}{\hat{\lambda}(\mu)} = -\frac{\beta_1}{\beta_0} \ln[\beta_0 \hat{\lambda}(\mu)] + \beta_0 (C - \ln(\mu a)) \; . \tag{2.20}$$

For Higgs- and Goldstone-boson scattering at $\sqrt{s} = a^{-1}$, our scale corresponds to $\mu = a^{-1}/e$; for $\sqrt{s} = 2a^{-1}$ (the approximate upper bound on the cutoff), it corresponds to $\mu = 2a^{-1}/e$. Solving for the coupling using Eq. (2.20), we find $\lambda(a^{-1}/e) = 2.7$, and $\lambda(2a^{-1}/e) = 3.5$. These values are comfortably below the value $\lambda(\sqrt{s}/e) = 4.0$ at which perturbation theory becomes unreliable.

We therefore conclude that the standard Higgs model is not strongly interacting at energies above the Higgs mass but below the cutoff. This is a new result, and complements the result that the Higgs model cannot be strongly interacting at energies of the order of the Higgs mass [6,7].

III. HIGGS DECAY

We now consider the decay amplitude of a heavy Higgs boson. This is another process which has been calculated at next-to-next-to-leading order [18,19], and therefore can also be used to explore the convergence of perturbation theory at large coupling. In contrast to Higgs- and Goldstone-boson scattering, however, the appropriate scale for the running coupling is the Higgs mass, $\mu = m_R$, not m_R/e. Since the energy entering the decay amplitude is the Higgs mass, one cannot neglect the Higgs mass in the loop diagrams. Thus the logarithms, which come predominantly from loops containing Higgs bosons, are not accompanied by the universal constant 2 associated with massless bubble diagrams, in contrast to the case

of high-energy scattering processes. Recall that this is the same reason the logarithms in the scattering counterterms are not accompanied by a universal constant.

Let us consider the maximum allowable Higgs mass, since this yields the maximum value of the coupling. Traditionally, this has been obtained from lattice calculations with the requirement that the cutoff be substantially greater than the Higgs mass. Recall that, for example, the upper bound on the coupling of $\lambda(m_R) = 3.2$ (requiring $a^{-1} > 2m_R$) obtained by Lüscher and Weisz translates into an upper bound of 630 GeV [6]. The analysis of Ref. [4] yields a similar bound of 680 GeV, using the same lattice action. We consider $m_R = 700$ GeV, which corresponds to a coupling $\lambda(m_R) = 4.0$. Based on our experience with Higgs- and Goldstone-boson scattering, we expect this value to lie just within the perturbative regime.

Written in terms of the running coupling $\lambda(\mu)$, the decay amplitude to a pair of Goldstone bosons [18,19] becomes [11]:

$$A(H \to ww) = -2v\lambda(\mu)\left[1 + \frac{\lambda(\mu)}{16\pi^2}\left[12\ln\frac{m_R^2}{\mu^2} + 1.40 - 3.61i\pi\right] + \left(\frac{\lambda(\mu)}{16\pi^2}\right)^2\left[144\ln^2\frac{m_R^2}{\mu^2} + (-122.4 - 86.73i\pi)\ln\frac{m_R^2}{\mu^2} - 34.35 - 21.00i\right]\right] . \tag{3.1}$$

We show in Fig. 4 the real and imaginary parts of the leading-order, next-to-leading order, and next-to-next-to-leading-order decay amplitude for $m_R = 700$ and 900 GeV, as a function of μ/m_R. In the case of 700 GeV (top figures), the amplitude is rather insensitive to the scale in the vicinity of $\mu = m_R$, while it is rather sensitive to the scale above and below this region. This supports our statement that the appropriate scale for the Higgs decay amplitude is indeed the Higgs mass. The sensitivity of the amplitude to the scale decreases with increasing order in perturbation theory for $\mu = m_R$, indicating that perturbation theory is reliable. Given the size of the coupling, the corrections to the decay amplitude are remarkably small, a feature we also observed in the case of Higgs- and Goldstone-boson scattering. The case of 900 GeV (bottom figures in Fig. 4) corresponds to a coupling $\lambda(m_R) = 6.7$, which is quite large. The scale dependence of the amplitude has significantly increased when compared with

the case of 700 GeV. The numerical studies of [11], which investigate the scale dependence of the decay *width* rather than the amplitude, find the perturbative approach to be unreliable for $m_R \gtrsim 700$ GeV. All these findings confirm that the maximal value of m_R found in lattice studies is within the perturbative range, supporting the original work of Lüscher and Weisz.

In Ref. [5,20] it is speculated that perturbation theory seriously underestimates the Higgs width for large Higgs mass, $m_R \approx 700$ GeV. This is based on a calculation of the Higgs width in the $1/N$ expansion. It is difficult to reconcile this with the fact that perturbation theory is apparently reliable for such a Higgs mass as seen in recent two-loop calculations [18,19]. The discrepancy with the $1/N$ calculation disappears when the Goldstone bosons are given a significant mass. The Higgs width on the lattice [21] (which is calculated with a significant Goldstone-boson mass $\sim m_R/3$) also suggests agreement with perturbation theory for a Higgs mass of roughly 700 GeV [19]. An extrapolation of the lattice results to the limit of (nearly) massless Goldstone bosons, as in the perturbative calculations, would be of interest.

IV. PHENOMENOLOGICAL IMPLICATIONS

If and when a Higgs boson is discovered, it will be interesting to measure vector-boson scattering at energies above the Higgs resonance. In the standard model, the Higgs boson is responsible for regulating the growth of the amplitude for longitudinal-vector-boson scattering with energy: At low energies, the scattering amplitude is proportional to s/v^2; above the resonance, it is proportional to λ. Observing this behaviour experimentally will be challenging.

As an example we look at the effect of our summation procedure on the case of high-energy $W^+W^- \to ZZ$ scattering. This process is of interest for future colliders such as the LHC or linear e^+e^- and $\mu^+\mu^-$ colliders. Its amplitude is immediately given by the generic amplitude $a(s,t,u)$; recall Eq. (2.4). Using the two-loop result of [9], the NNLL cross section with its explicit μ dependence is [11]

$$\sigma(s) = \frac{1}{8\pi s}[\lambda(\mu)]^2 \left[1 + \left(24 \ln \frac{s}{\mu^2} - 42.65 \right) \frac{\lambda(\mu)}{16\pi^2} \right.$$

$$+\left(432\ln^2\frac{s}{\mu^2}-1823.3\ln\frac{s}{\mu^2}+\ 2457.9\right)\frac{\lambda^2(\mu)}{(16\pi^2)^2}\ +\ \mathrm{O}\left(\lambda^3(\mu)\right)\Bigg], \quad (4.1)$$

where the anomalous dimension prefactor has been neglected since it is close to unity for the values of $\sqrt{s}$ and m_R considered here. Thus the product $s\sigma$ depends only on the three-loop running coupling and the ratio $\mu/\sqrt{s}$.

In Fig. 5 we show $s\sigma$ as a function of $\mu/\sqrt{s}$, fixing the running coupling such that $\lambda(\mu = \sqrt{s}/e)$ is equal to 1.5. Using the scale $\mu = \sqrt{s}/e$, we find the size of the radiative corrections to be significantly reduced. In addition, the reduced scale dependence around $\mu = \sqrt{s}/e$ is clearly visible. The leading-log approximation with the conventional scale $\mu = \sqrt{s}$ overestimates the magnitude of the cross section by more than 30%, whereas the scale $\mu = \sqrt{s}/e$ yields a leading-log result only slightly less than the NLL and NNLL results. We conclude that phenomenological studies based on tree-level results are much more reliable when using $\mu = \sqrt{s}/e$.

Fixing $\mu = \sqrt{s}/e$, we show in Fig. 6 the LL, NLL, and NNLL result for $s\sigma$ as a function of $\lambda(\sqrt{s}/e)$, displaying the perturbative range $0.5 < \lambda(\sqrt{s}/e) < 3.5$. Using Table I, the value of the running coupling can be related to the desired Higgs mass and the center-of-mass energy of the incoming W_LW_L pair. Standard analyses of the cross section using $\mu = \sqrt{s}$ lead to large uncertainties [10] for running coupling larger than about 2. The improved scale greatly reduces the one-loop and two-loop corrections, allowing for predictive cross sections even for $\lambda(\sqrt{s}/e)$ close to 4.

The high-energy amplitude given here is completely based on the four-point interactions of the Higgs sector, a good approximation for $\sqrt{s} > 2 - 3m_R$ [10]. For smaller values of $\sqrt{s}$, the three-point interactions dominate over the four-point coupling. In addition, the electroweak gauge couplings contribute to the cross section, making a measurement of the Higgs coupling difficult.

V. CONCLUSIONS

In this paper we resolve the mystery, raised in Ref. [8] and deepened in Refs. [9–11], that the perturbative calculation of Higgs- and Goldstone-boson scattering, at energies large compared with the Higgs mass, is apparently unreliable for rather small values of the running coupling, $\lambda = 2.0 - 2.3$. The resolution lies in the choice of the scale in the running coupling $\lambda(\mu)$. All previous analyses have implicitly or explicitly used $\mu = \sqrt{s}$. We argue that a more appropriate scale is $\mu = \sqrt{s}/e$, and show that this scale leads to a dramatic improvement in the convergence of perturbation theory for Higgs- and Goldstone-boson scattering. We find that perturbation theory is apparently reliable up to a coupling $\lambda \approx 4$, consistent with the perturbative unitarity bound of $\lambda < 4\pi/3 \approx 4.2$.

With the improved perturbation theory, we address the question of whether Higgs- and Goldstone-boson scattering can become strongly interacting at energies above the Higgs mass but below the cutoff, modeled by the inverse lattice spacing. We find that the value of the coupling for Higgs- and Goldstone-boson scattering at the cutoff is within the perturbative domain: a strongly-interacting standard Higgs model at high energies is excluded. This is a new result, and complements the result that the Higgs sector cannot be strongly interacting at energies near the Higgs mass [6,7].

We also consider the decay amplitude of the Higgs boson to Goldstone bosons. In this case we argue that the appropriate scale is the Higgs mass, and we show that perturbation theory is apparently reliable up to a coupling of $\lambda(m_R) = 4.0$, which corresponds to a Higgs mass of 700 GeV. This supports the conclusions of Ref. [6,7]. This is difficult to reconcile with the observation, made in Ref. [5], that there is a discrepancy between the Higgs width calculated in the $1/N$ expansion and in perturbation theory for $m_R \approx 700$ GeV. A lattice calculation of the Higgs width with an extrapolation to the case of (nearly) massless Goldstone bosons would be desirable.

The most important aspect of our work is the realization that the apparent breakdown of perturbation theory at weak coupling is simply due to a poor choice of scale in the running

coupling. Our argument for the scale $\mu = \sqrt{s}/e$ is based on an analysis of the constant which accompanies the logarithm in the one-loop bubble diagram. It may be possible to refine this argument further. One might be able to develop a scale-fixing scheme analogous to the BLM method [22]: the number of Goldstone bosons, n_g, could play the role of n_f, the number of light fermions. (The terms proportional to n_g connected to the counterterms should not be included in a BLM analysis.) Naively applying the BLM method at one loop leads to the same scale which we advocate. It is also interesting that our scale lies in the region where the amplitude is quite insensitive to the choice of scale. Therefore the principle of minimal sensitivity [23] is also expected to lead to a scale close to $\mu = \sqrt{s}/e$.

ACKNOWLEDGMENTS

We are grateful for conversations and correspondance with M. Beneke, A. El-Khadra, U. Heller, P. Mackenzie, M. Neubert, U. Nierste, and P. Weisz. This work was performed in part at the Aspen Center for Physics. S. W. was supported in part by Department of Energy grant DE-FG02-91ER40677.

APPENDIX A: RELATION OF M_R TO THE HIGGS BOSON MASS M_H

The quantity m_R^2 is defined as the zero of the real part of the inverse Higgs-boson propagator. A physical definition of the Higgs mass, m_H, is the real part of the pole (in the energy plane) of the Higgs propagator [6,24]. This definition is process-independent and field-redefinition invariant. The relation between m_R and m_H is

$$m_H^2 = m_R^2 \left[1 + \frac{\Gamma_H^2}{4} + \cdots \right] = m_R^2 \left[1 + \frac{9}{64} \left(\frac{\lambda(m_R)}{4\pi} \right)^2 + \cdots \right] , \tag{A1}$$

where Γ_H is the Higgs width. The $\mathcal{O}(\lambda^3)$ term in Eq. (A1) is given in Ref. [24]. For $m_R \leq 1200$ GeV, the distinction between m_R and m_H is numerically negligible, so one may safely refer to m_R as the physical Higgs mass.

APPENDIX B: THE RUNNING COUPLING $\lambda(\mu)$ AND THE β FUNCTION TO THREE LOOPS

To obtain renormalization-group-improved scattering amplitudes, the evolution of $\lambda(\mu)$ as a function of μ is needed. It is dictated by the renormalization group equation,

$$\frac{d\lambda(\mu)}{d\ln\mu} = \beta(\lambda(\mu)) \,, \tag{B1}$$

with the initial condition imposed by Eq. (2.3). For large values of λ we can neglect all gauge and Yukawa coupling contributions to the beta function. The three-loop result is [7,11]:

$$\beta(\lambda) = 24\frac{\lambda^2}{16\pi^2}\left[1 - 13\frac{\lambda}{16\pi^2} + 176.6\left(\frac{\lambda}{16\pi^2}\right)^2\right] \,. \tag{B2}$$

Neglecting the appropriate powers of λ, these equations determine the n-loop running coupling for $n \leq 3$. Explicitly, the one-loop running coupling is

$$\lambda(\mu) = \frac{\lambda(m_R)}{1 - 12\,\frac{\lambda(m_R)}{16\pi^2}\ln\left(\frac{\mu^2}{m_R^2}\right)} \,. \tag{B3}$$

At higher order the solution of Eq. (B1) is not unique anymore, and various solutions are discussed in [11]. We take the "consistent solution" introduced in [11]. The n-loop running coupling sums the leading logs, next-to-leading logs, and next-to-next-to-leading logs of the physical amplitudes for $n = 1, 2, 3$, respectively.

APPENDIX C: NONZERO HIGGS MASS EFFECTS IN THE BUBBLE DIAGRAM

The Feynman amplitude for Higgs- and Goldstone-boson scattering receives contributions from the *massless* scalar bubble diagram,

$$B(p^2) \equiv B_0(p^2; m_1^2 = 0, m_2^2 = 0) = \frac{1}{\epsilon} - \gamma + \ln\left(\frac{4\pi\mu^2}{-p^2}\right) + 2 + O(\epsilon) \tag{C1}$$

where p is the incoming four-momentum, and m_1, m_2 are the internal particle masses. The logarithm is accompanied by the constant 2. In the limit $p^2 \gg m_R^2$, the bubble diagrams with internal Higgs propagators ($m_1^2 = m_2^2 = m_R^2$) are also well approximated by the massless case

$B(p^2)$. The counterterms appearing in Eq. (2.11) receive contributions from bubble diagrams with $p^2 = 0$ or m_R^2: the masses of the internal Higgs bosons cannot be neglected, and the corresponding finite pieces are different from 2. To illustrate this we list the different bubble contributions occuring at one loop:

$$B_0(m^2;0,0) = \frac{1}{\epsilon} - \gamma + \ln\left(\frac{4\pi\mu^2}{m^2}\right) + 2 + i\pi + O(\epsilon)\,, \tag{C2}$$

$$B_0(m^2;m^2,m^2) = \frac{1}{\epsilon} - \gamma + \ln\left(\frac{4\pi\mu^2}{m^2}\right) + 2 - \frac{\pi}{\sqrt{3}} + O(\epsilon)\,, \tag{C3}$$

$$B_0(0;0,m^2) = \frac{1}{\epsilon} - \gamma + \ln\left(\frac{4\pi\mu^2}{m^2}\right) + 1 + O(\epsilon)\,, \tag{C4}$$

APPENDIX D: THE TWO-LOOP SCATTERING GRAPHS

At two loops, the only relevant high-energy scattering topologies are $A(p^2)$ and $[B(p^2)]^2$. Their exact results are given in [14]. Expanding in powers of ϵ and neglecting $O(\epsilon)$ terms, they are evaluated as:

$$A(p^2) = \frac{(4\pi e^{-\gamma})^{2\epsilon}}{(4\pi)^4}\left(\frac{\mu^2}{-p^2}\right)^{2\epsilon}\left(\frac{1}{2\epsilon^2} + \frac{5}{2\epsilon} + \frac{19}{2} + \frac{1}{2}\zeta(2) + O(\epsilon)\right)\,, \tag{D1}$$

$$\left[B(p^2)\right]^2 = \frac{(4\pi e^{-\gamma})^{2\epsilon}}{(4\pi)^4}\left(\frac{\mu^2}{-p^2}\right)^{2\epsilon}\left(\frac{1}{\epsilon^2} + \frac{4}{\epsilon} + 12 - \zeta(2) + O(\epsilon)\right)\,. \tag{D2}$$

APPENDIX E: SUMMING POWERS OF THE BUBBLE DIAGRAM

The scale $\mu = \sqrt{s}/e$ is motivated by the summation of the contribution 2^n which comes from the $[B(p^2)]^n$ terms at n loops. Since $B(p^2)$ is ultraviolet divergent, the $O(\epsilon^m)$ terms will also contribute at orders $n > m \geq 0$. Here we show that the improved scale also sums those contributions partially, at least as checked up to $n = 5$ loops. The exact result of $B(p^2)$ to all orders in ϵ is

$$B(p^2) = \frac{(4\pi e^{-\gamma})^{\epsilon}}{16\pi^2}\left(\frac{\mu^2}{-p^2}\right)^{\epsilon}\frac{1}{\epsilon\,(1-2\epsilon)}\,\exp\left\{\sum_{n=2}^{\infty}\frac{\epsilon^n\zeta(n)}{n}\left[2 - 2^n + (-1)^n\right]\right\}\,, \tag{E1}$$

where ζ is the Riemann Zeta function. Expanding up to $O(\epsilon^4)$ yields the numerical result

$$B(p^2) = \frac{(4\pi e^{-\gamma})^\epsilon}{16\pi^2}\left(\frac{\mu^2}{-p^2}\right)^\epsilon \times \left(\frac{1}{\epsilon} + 2 + 3.1775\epsilon + 3.5502\epsilon^2 + 3.9212\epsilon^3 + 3.7203\epsilon^4 + O(\epsilon^5)\right) . \quad \text{(E2)}$$

The $O(\epsilon^{n-1})$ term of this expansion contributes to the finite part of the perturbative amplitude at n loops and even higher orders. Factoring out the constant 2 which is summed by the scale choice $\mu = \sqrt{s}/e$, we find that the coefficients of the power series in ϵ of the previous equation are reduced in magnitude:

$$B(p^2) = \frac{(4\pi e^{-\gamma})^\epsilon}{16\pi^2}\left(\frac{e^2\mu^2}{-p^2}\right)^\epsilon \times \left(\frac{1}{\epsilon} + 0 + 1.1775\epsilon - 0.1381\epsilon^2 + 1.1757\epsilon^3 - 0.1916\epsilon^4 + O(\epsilon^5)\right) . \quad \text{(E3)}$$

It is also possible to completely cancel the coefficients to all orders using the G scheme [25].

REFERENCES

[1] S. Weinberg, Phys. Rev. Lett. **19**, 1264 (1967); A. Salam, in *Elementary Particle Theory: Relativistic Groups and Analyticity (Nobel Symposium No. 8)*, edited by N. Svartholm (Almqvist and Wiksell, Stockholm, 1968), p. 367.

[2] This is related to the "triviality" of scalar field theory. For a review see: *The Standard Model Higgs Boson*, ed. M. Einhorn, Current Physics Sources and Comments, Vol. 8 (North-Holland, Amsterdam, 1991).

[3] R. Dashen and H. Neuberger, Phys. Rev. Lett. **50**, 1897 (1983).

[4] M. Göckeler, H. Kastrup, T. Neuhaus, and F. Zimmermann, Nucl. Phys. **B404**, 517 (1993).

[5] U. Heller, M. Klomfass, H. Neuberger, and P. Vranas, Nucl. Phys. **B405**, 555 (1993).

[6] M. Lüscher and P. Weisz, Phys. Lett. **B212**, 472 (1988).

[7] M. Lüscher and P. Weisz, Nucl. Phys. **B318**, 705 (1989).

[8] L. Durand, J. Johnson, and J. Lopez, Phys. Rev. Lett. **64,**, 1215 (1990); Phys. Rev. D **45**, 3112 (1992).

[9] L. Durand, P. Maher, and K. Riesselmann, Phys. Rev. D **48**, 1084 (1993).

[10] K. Riesselmann, Phys. Rev. D **53**, 6226 (1996).

[11] U. Nierste and K. Riesselmann, Phys. Rev. D **53**, 6638 (1996).

[12] D. Dicus and V. Mathur, Phys. Rev. D **7**, 3111 (1973).

[13] B. Lee, C. Quigg, and H. Thacker, Phys. Rev. D **16**, 1519 (1977).

[14] P. Maher, L. Durand, and K. Riesselmann, Phys. Rev. D **48**, 1061 (1993); (E) **52**, 553 (1995).

[15] W. Marciano and S. Willenbrock, Phys. Rev. D **37**, 2509 (1988).

[16] A. Ghinculov, Phys. Lett. **B337**, 137 (1994); (E) **346**, 426 (1995).

[17] W. Marciano, G. Valencia, and S. Willenbrock, Phys. Rev. D **40**, 1725 (1989).

[18] A. Ghinculov, Nucl. Phys. **B455**, 21 (1995).

[19] A. Frink, B. Kniehl, D. Kreimer, and K. Riesselmann, TUM-HEP-247/96 (1996) and hep-ph/9606310; to appear in PRD.

[20] U. Heller, H. Neuberger, and P. Vranas, Nucl. Phys. **B399**, 271 (1993).

[21] M. Göckeler, H. Kastrup, J. Westphalen, and F. Zimmermann, Nucl. Phys. **B425**, 413 (1994).

[22] S. Brodsky, P. Lepage, and P. Mackenzie, Phys. Rev. D **28**, 228 (1983).

[23] P. Stevenson, Phys. Rev. D **23**, 2916 (1981); Nucl. Phys. **B203**, 472 (1982).

[24] G. Valencia and S. Willenbrock, Phys. Lett. **B247**, 341 (1990).

[25] K.G. Chetyrkin, A.L. Kataev, and F.V. Tkachov, Nucl. Phys. **B174**, 345 (1980).

TABLES

TABLE I. Relating the values of $\lambda(\sqrt{s}/e)$ to $\lambda(\sqrt{s})$ using the three-loop renormalization-group equation. The initial condition on the running coupling is given by Eq. (2.3). Some representative values of corresponding pairs of $(m_R, \sqrt{s})$ are also given, requiring $\sqrt{s} > m_R$.

	$\lambda\,(\mu{=}\sqrt{s}/e)$ $\quad[\,\lambda\,(\mu{=}\sqrt{s})\,]$					
	0.50 [0.54]	1.0 [1.2]	2.0 [2.7]	3.0 [4.6]	4.0 [7.0]	5.0 [9.8]
m_R (GeV)	$\sqrt{s}$ (GeV)					
250	4.4 E 02	4.6 E 05	1.8 E 07	6.7 E 07	1.3 E 08	2.1 E 08
300	–	9.3 E 03	3.6 E 05	1.3 E 06	2.7 E 06	4.2 E 06
350	–	8.7 E 02	3.4 E 04	1.3 E 05	2.6 E 05	4.0 E 05
400	–	–	7.3 E 03	2.7 E 04	5.5 E 04	8.6 E 04
500	–	–	1.2 E 03	4.5 E 03	9.0 E 03	1.4 E 04
600	–	–	–	1.7 E 03	3.4 E 03	5.3 E 03
700	–	–	–	9.2 E 02	1.9 E 03	2.9 E 03
800	–	–	–	–	1.3 E 03	2.0 E 03
900	–	–	–	–	9.6 E 02	1.5 E 03
1000	–	–	–	–	–	1.2 E 03

FIGURES

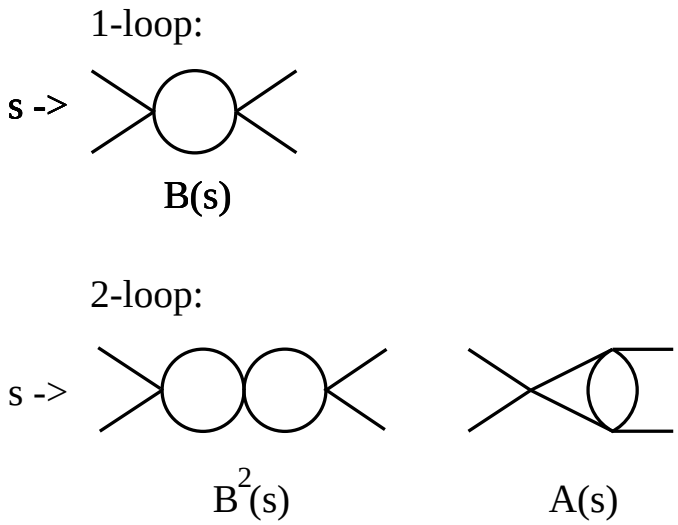

FIG. 1. Topologies of s-channel Feynman diagrams contributing to Higgs- and Goldstone-boson scattering at one and two loops. The t- and u-channel diagrams are obtained by crossing relations.

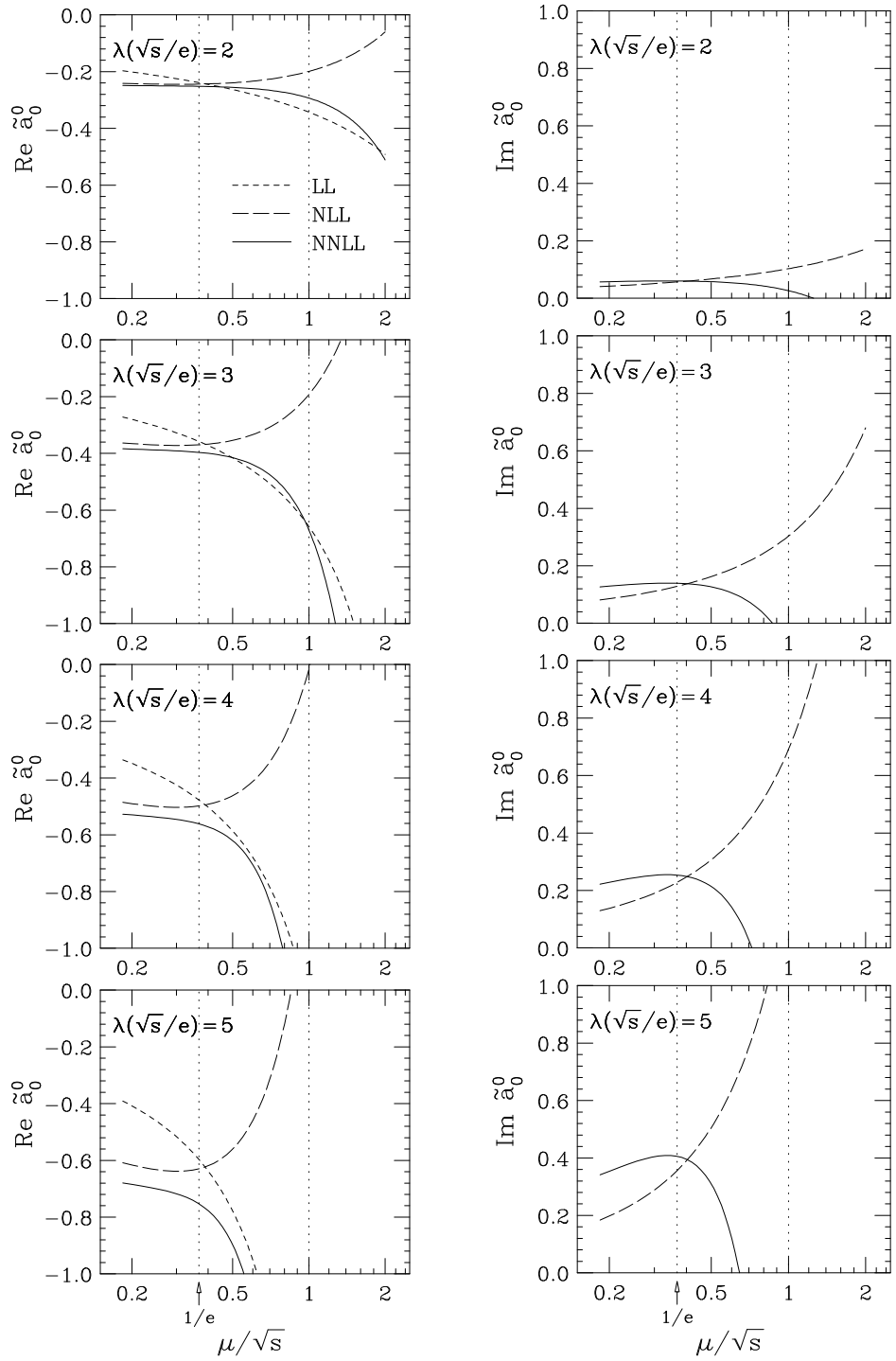

FIG. 2. Real part (left column) and imaginary part (right column) of the LL, NLL, and NNLL $J = 0$ eigenamplitude, $\tilde{a}_0^0$, for Higgs- and Goldstone-boson scattering. The amplitude is shown as a function of $\mu/\sqrt{s}$, fixing $\lambda(\sqrt{s}/e)$ to be 2.0, 3.0, 4.0, and 5.0 (from top to bottom). The corresponding values of $\lambda(\sqrt{s})$ are 2.7, 4.6, 7.0, and 9.8.

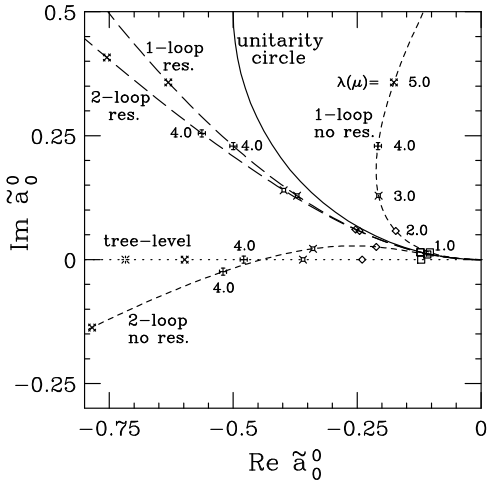

FIG. 3. The real and imaginary part of the eigenamplitude $\tilde{a}_0^0$ plotted in an Argand diagram. Shown are the NLL and NNLL results with (long dashes) and without (short dashes) summation of the constant 2. The curves are parameterized as a function of the running coupling $\lambda(\mu)$, so the LL results (dotted curve) coincide in the two approaches.

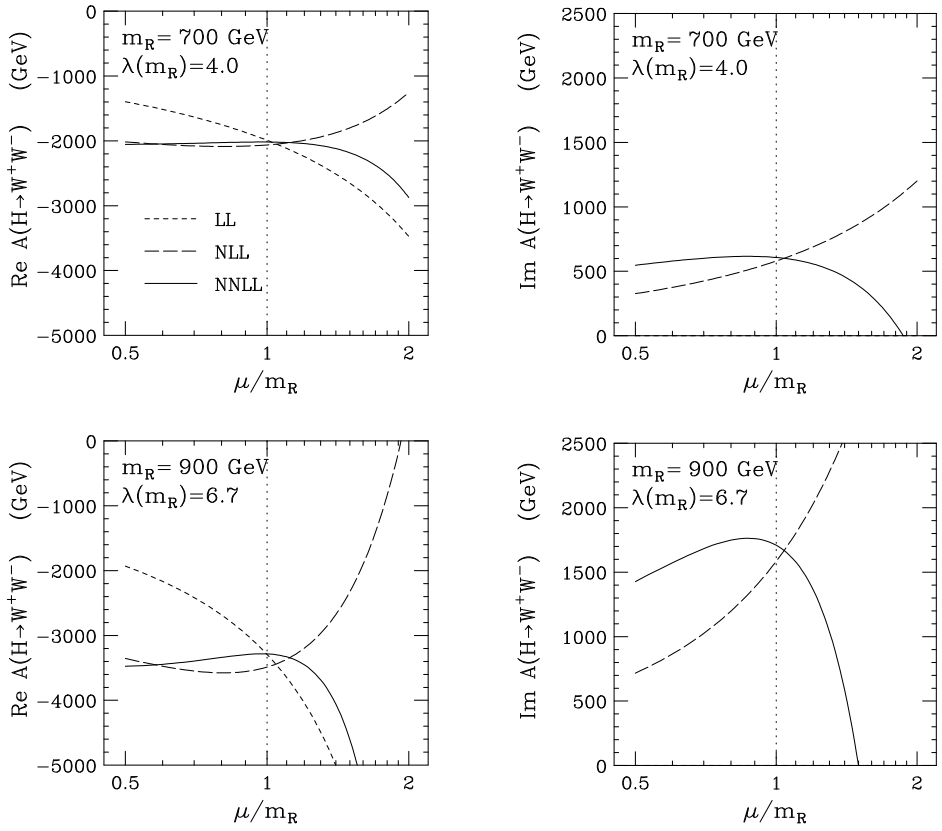

FIG. 4. Real and imaginary parts of the leading order, next-to-leading order, and next-to--next-to-leading order amplitude for Higgs decay to a pair of Goldstone bosons as a function of μ/m_R, for $m_R = 700$ and 900 GeV.

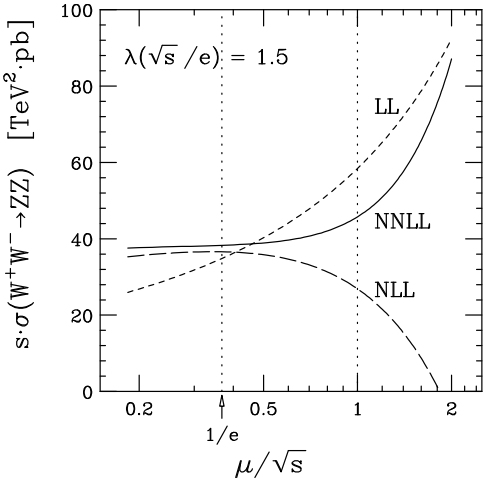

FIG. 5. The μ-dependence of the scaled cross section of $W_L^+W_L^- \to Z_LZ_L$ for $\lambda(\sqrt{s}/e) = 1.5$ in the high-energy approximation. Gauge and Yukawa coupling contributions are neglected.

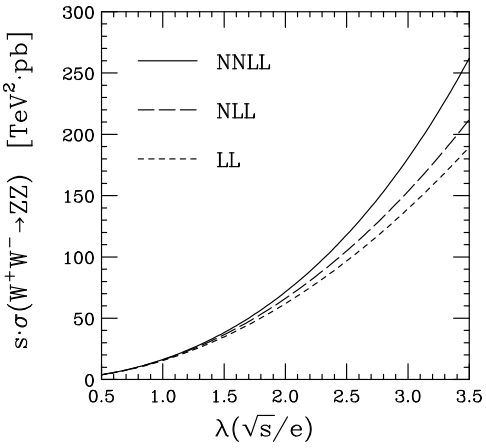

FIG. 6. The scaled cross section of $W_L^+W_L^- \to Z_LZ_L$ for $0.5 < \lambda < 3.5$ in the high-energy approximation, fixing $\mu = \sqrt{s}/e$. Gauge and Yukawa coupling contributions are neglected. The values of $\lambda(\sqrt{s}/e)$ can be converted to $(m_R, \sqrt{s})$ using Table I.